Frequency tunable terahertz metamaterials using broadside coupled split-ring resonators

E. Ekmekci, A. C. Strikwerda, K. Fan, G. Keiser, X. Zhang, G. Turhan-Sayan, and R. D. Averitt

Frequency-tunable terahertz metamaterials using broadside-coupled split ring resonators

E. Ekmekci[1, 3, 4], A. C. Strikwerda[1], K. Fan[2], G. Keiser[1], X. Zhang[2], G. Turhan-Sayan[3], and R. D. Averitt[1]

[1]Boston University, Department of Physics, Boston, MA 02215, USA
[2]Boston University, Department of Mechanical Engineering, Boston, MA 02215, USA
[3]Middle East Technical University, Department of Electrical and Electronics Engineering, 06531, Ankara, Turkey
[4]Suleyman Demirel University, Department of Electronics and Communication Engineering, 32260, Isparta, Turkey

We present frequency tunable metamaterial designs at terahertz (THz) frequencies using broadside-coupled split ring resonator (BC-SRR) arrays. Frequency tuning, arising from changes in near field coupling, is obtained by in-plane displacement of the two SRR layers. For electrical excitation, the resonance frequency continuously redshifts as a function of displacement. The maximum frequency shift occurs for vertical displacement of half a unit cell, resulting in a shift of 663 GHz (51% of f_0). We discuss the difference in BC-SRR response for electrical excitation in comparison to magnetic excitation in terms of hybridization arising from inductive and capacitive coupling.

Across the spectrum, electromagnetic metamaterials research continues to blossom with a significant fraction of work focusing on split ring resonators (SRRs) [1] and their variants which includes, as examples, spiral [2], labyrinth [3], and electric field coupled (ELC) resonators [4]. It is well known that metamaterials can provide a μ-negative (MNG) and/or ε-negative (ENG) response. However, these operational MNG/ENG bands are limited to a narrow spectral region. Frequency tunable metamaterials have become an important area of interest since tuning the resonance frequency (f_0) can effectively extend the operating bandwidth for certain applications.

Numerous approaches to modify the electromagnetic response of metamaterials (i.e. frequency and/or amplitude of the resonance) have been considered. This includes modification of the substrate parameters (i.e. thickness and permittivity) [5-7], the use of liquid crystals [8], lumped capacitors or varactors [9], ferromagnetic [10, 11] and ferroelectric [12, 13] techniques, semiconductors [14-16], microelectromechanical (MEMS) switches [17-19], and tuning based on near-field interactions between adjacent SRRs [20-25]. This last approach is the topic of the present study.

Wang *et al.* proposed tuning the electromagnetic response in the microwave region through sub-unit cell relative displacements between the two layers (Fig. 1b) comprising a broadside-coupled SRR (BC-SRR) structure under magnetic excitation [22]. They showed that displacement resulted in a capacitive change yielding a shift in f_0. This work on structural tuning through in-plane displacement was continued in and generalized in [24]. The definition of in-plane horizontal and vertical displacement of the two layers comprising the BC-SRR array is depicted in Fig. 1c and 1d. Importantly, these results all utilized magnetic excitation at microwave frequencies, and observed a blueshift of the fundamental resonance.

In this paper, we investigate the effects of lateral shifting of broadside coupled metamaterials at THz frequencies under electrical excitation (Fig 1a). In [24], Powell et al., predicted a higher frequency mode, with low coupling efficiency, that would redshift with offset, but its response was small compared with the fundamental magnetic resonance. Through a judicious choice of geometry and excitation, we have excited this mode exclusively. To illustrate this, we design, fabricate, and characterize a two-layered terahertz (THz) SRR array with different lateral shifts between layers. The BC-SRR arrays are characterized experimentally using THz time-domain spectroscopy (THz-TDS) and modeled using CST Microwave Studio. Of greatest significance is that for electrical excitation, the fundamental resonance frequency continuously *redshifts* as a function of displacement in

contradistinction to magnetic excitation. The maximum frequency shift occurs for displacement of half a unit cell, resulting in an experimental shift of 663 GHz (51% of f_0). We present an intuitive description of changes in coupling in BC-SRRs as a function of displacement to provide insight into the different electromagnetic responses under electrical and magnetic excitation.

It is well known that single SRRs can be excited with either the magnetic or electric component of the incident radiation and that the LC resonance frequency for these two cases is degenerate. The primary motivation for creating broadside coupled resonators is that bianisotropy is eliminated at the unit cell level and, for magnetic excitation, strong coupling between the two split rings decreases the resonance frequency and reduces the dimensions of the particle with respect to the wavelength. More generally, the broadside orientation leads to maximal coupling between the resonators. This creates a strong hybridization resulting in a splitting of the mode degeneracy. When compared to a single resonator, the magnetically excited mode redshifts and the electrically excited resonance blueshifts. This hybridization picture is summarized in Fig. 2.

To provide further insight into the resonance hybridization in BC-SRR structures, we qualitatively examine the current and charge distributions of the top and bottom layers of a single unit cell under electrical and magnetic excitation. In the following discussion, we consider exclusively the LC resonance where $f_0 \sim (L_{total} C_{total})^{-1/2}$ (i.e. not the higher frequency dipolar resonances). We also neglect lattice effects since previous work [24] and our simulations (not shown for brevity) indicate that intra-cell coupling is the dominant effect. Fig. 3a shows that for magnetic excitation, the surface currents of the top and bottom layers are in the same direction (symmetric). This results in a mutual inductance (L_{mut}) with a positive sign yielding a total inductance $L_{total} = L_{self} + L_{mut}$. For electrical excitation (Fig. 3b), the surface currents are in the opposite directions (antisymmetric) meaning that L_{mut} is

negative resulting in a total inductance $L_{total} = L_{self} - L_{mut}$. Lateral shifts between the top and bottom layers reduce the coupling and therefore the hybridization. Lateral shifts can be in the horizontal or vertical direction (Fig. 1c and 1d) either of which will decrease/increase L_{total} under magnetic/electrical excitation.

Similarly, the surface charge distribution and subsequent mutual capacitance depends on the excitation conditions. For magnetic excitation, positive and negative charges between the two layers overlap resulting in a significant mutual capacitance. While this description is qualitative, it shows that, under magnetic excitation, lateral shifting (either horizontal or vertical) decreases the inductance and capacitance consistent with the blueshift observed in the previous work [24] and consistent with the hybridization point-of-view depicted in Fig. 2.

In contrast, for electrical excitation (Fig. 3b), negative charges overlap with negative and positive with positive between the two layers yielding a much weaker mutual capacitance. Importantly, changes in the mutual capacitance, unlike the mutual inductance, are sensitive to the shift direction. For vertical shifting, the positive and negative charged arms between the upper and lower layers of adjacent unit cells come closer (i.e. total overlap for a shift of ½ a unit cell) leading to an increased mutual capacitance. However, for horizontal shifting, the SRR arrays slide over the SRR arms with charges of the same sign providing a smaller change in the mutual capacitance. This suggests a greater frequency shift for vertical displacement in comparison to horizontal displacement under electrical excitation, which we have confirmed in both simulation and experiment. However, for brevity, we limit our analysis solely to vertically shifted BC-SRR arrays. It is clear that for electrical excitation, lateral displacement should lead to redshifting of the LC resonance since both the capacitance and inductance increase.

To verify changes in the resonant response as a function of lateral displacement under electrical excitation, we fabricated structures composed of square shaped SRR unit-cells

having the same physical dimensions as shown schematically in Fig. 1e. The unit-cell periodicity is P=60μm, metallization side-length l=40μm, metallization width w=11μm, gap width g=5μm. This choice of dimensions means that a 30μm shift creates a perfect overlap between legs of a top layer SRR with the legs of two bottom layer SRRs in adjacent unit cells.

The structures were fabricated using conventional photolithography. For all structures, 5μm of polyimide was spin-coated on GaAs as a superstrate and then 200nm thick gold with a 10nm thick adhesion layer of titanium is deposited on a resist layer (S1813, Shipley) and patterned to form a planar array of SRR structures. Another 4μm thick polyimide layer was then coated on the SRR array as the spacer. Next, the second planar array of SRRs was patterned to form a BC-SRR structure. Finally, a 5μm thick polyimide was coated on metamaterials as the second superstrate (Fig. 1f). The multi-layer structure was removed from the GaAs resulting in a thin metamaterial film with a total thickness of 14μm. The polyimide (PI-5878G, HD MicrosystemsTM) has the relative permittivity (ε_r) of 2.88 and the dielectric loss-tangent of (tanδ_c=0.0313).

The fabricated samples were measured experimentally using THz-TDS and simulated with CST Microwave Studio. Optical microscope pictures of the shifted arrays and the corresponding simulation/experimental results are given in Fig. 4a and Fig. 4b/Fig. 4c, respectively. With increasing displacement, the resonance frequency decreases dramatically from 1.351 THz to 0.631 THz in simulation and, experimentally, from 1.304 THz to 0.641 THz. These results correspond to a 720 GHz absolute and 53% percentage shift in simulation and a 663 GHz absolute and 51% percentage shift in experiment.

The experimental results and full-wave simulations verify the previous discussion. For electrical excitation, lateral shifting alters the hybridization interactions and redshifts the resonance. We also note that as a function of shifting, there is a broadening of the transmission resonance. The analysis of this broadening (which arises from an increase in the

oscillator strength), along with an effective medium analysis will be presented in a subsequent publication.

Finally, it is worth noting that due to our geometry and excitation at normal incidence, these arrays couple solely to the electric field. It was shown in [24] that under magnetic excitation, shifted BC-SRR arrays would couple to both the electric and magnetic field. However, there is only 4μm of separation between the SRR arrays, and as a result, there is insufficient interaction length to excite the magnetic mode. To illustrate this further, we simulated the broadband transmission for shifts of 0μm to 30μm in steps of 0.5μm, which we have compiled in Fig. 5. As shown in [24], the magnetic mode, if present, would mirror the electric resonance about the vertical line $\omega/\omega_0 = 1$. The absence of this second curve clearly highlights that we have coupled solely to the electric response of these samples.

In conclusion, we have investigated the effect of near field coupling in electrically excited BC-SRR arrays. We have demonstrated an electrically excited structure that is amenable to creating mechanically actuated frequency agile metamaterials, demonstrated by an experimental resonance shift of over 50% of the center frequency. Further, we have highlighted the substantial differences in the electromagnetic response that arise for electrical excitation in comparison to magnetic excitation that naturally arise from hybridization. Our results demonstrate the use of structural tunability under electrical excitation, and highlight the significance of near field coupling of SRRs for future metamaterial applications.

support throughout the course of this research.

References

1. J. B. Pendry, A. J. Holden, D. J. Robbins, and W. J. Stewart, IEEE Trans. Microw. Theory Tech. **47**(11), 2075 (1999).
2. J. D. Baena, R. Marques, F. Medina, and J. Martel, Phys. Rev. B **69**, 014402 (2004).
3. I. Bulu, H. Caglayan, and E. Ozbay, Opt. Express **13**, 10238 (2005).
4. D. Schuring, J. J. Mock, and D. R. Smith, Appl. Phys. Lett. 88, 041109 (2006).
5. Z. Sheng, and V. V. Varadan, J. Appl. Phys. **101**(1), 014909 (2007).
6. E. Ekmekci, R. D. Averitt, G. Turhan-Sayan, PIERS Proceedings, Cambridge, USA, 538 (2010).
7. E. Ekmekci, and G. Turhan-Sayan, Prog. Electromagn. Res. B **12**, 35 (2009).
8. Q. Zhao, L. Kang, B. Du, B. Li, J. Zhou, H. Tang, X. Liang, and B. Zhang, Appl. Phys. Lett. **90**, 011112 (2007).
9. O. Reynet, and O. Acher, Appl. Phys. Lett. **84**, 1198 (2004).
10. L. Kang, Q. Zhao, H. Zhao, and J. Zhou, Opt. Express **16**, 8825 (2008).
11. D.-Y. Zou, A.-M. Jiang, and R.-X. Wu, J. Appl. Phys. 107, 013507 (2010).
12. T. H. Hand, and S. A. Cummer, J. Appl. Phys. **103**, 066105 (2008).
13. M. Gil, C. Damm, A. Giere, M. Sazegar, J. Bonache, R. Jakoby, and F. Martín, Electron. Lett. **45**, 417 (2009).
14. H. T. Chen, J. F. O'Hara, A. K. Azad, A. J. Taylor, R. D. Averitt, D. Shrekenhamer, and W. J. Padilla, Nat. Photonics **2**, 295 (2008).
15. K. A. Boulais, D. W. Rule, S. Simmons, F. Santiago, V. Gehman, K. Long, and A. Rayms-Keller, Appl. Phys. Lett. **93**, 043518 (2008).
16. J. Han, A. Lakhtakia, and C.-W. Qiu, Opt. Express **16**, 14390 (2008).
17. I. Gil, F. Martín, X. Rottenberg, and W. De Raedt, Electron. Lett. **43**, 1153 (2007).
18. T. Hand, and S. Cummer, IEEE Antennas Wirel. Propag. Lett. **6**(11), 401 (2007).
19. E. Ekmekci, K. Topalli, T. Akin, and G. Turhan-Sayan, Opt. Express 17, 16046 (2009).
20. M. Gorkunov, M. Lapine, E. Shamonina, and K. H. Ringhofer, Eur. Phys. J. B 28, 263 (2002).
21. I. V. Shadrivov, D. A. Powell, S. K. Morrison, Y. S. Kivshar, and G. N. Milford, Appl. Phys. Lett, 90, 201919 (2007).
22. J. Wang, S. Qu, J. Zhang, H. Ma, Y. Yang, C. Gu, and X. Wu, Prog. Electromagn. Res. Lett. 6, 35 (2009).
23. M. Lapine, D. Powell, M. Gorkunov, I. Shadrivov, R. Marqués, and Y. Kivshar, Appl. Phys. Lett. 95, 084105 (2009).
24. D. A. Powell, M. Lapine, M. V. Gorkunov, I. V. Shadrivov, and Y. S. Kivshar, Phys. Rev. B 82, 155128, (2010).
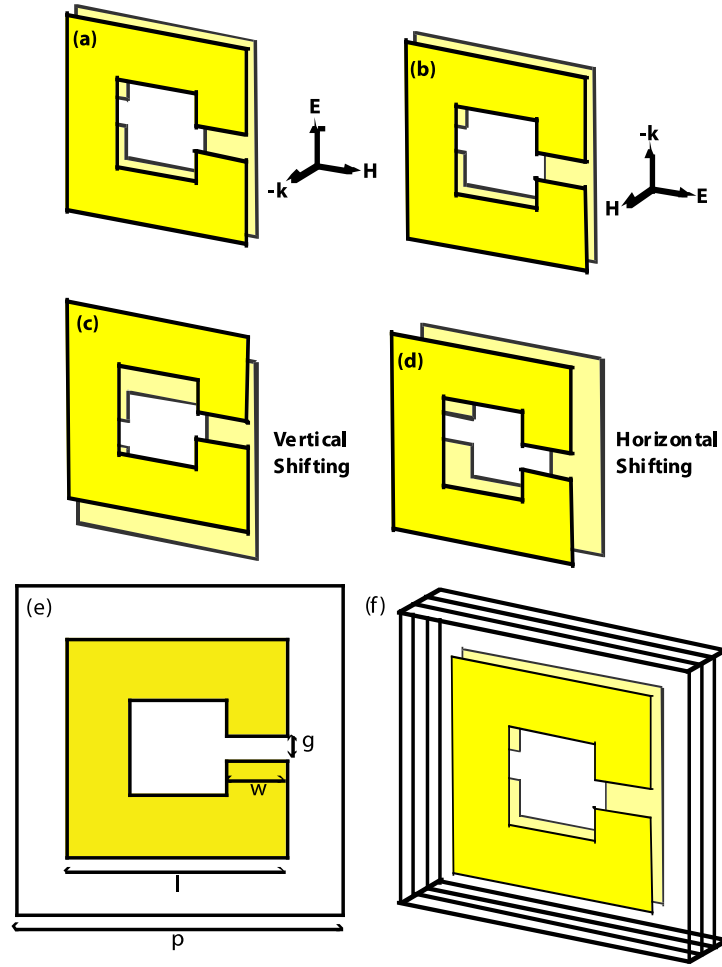25. N. Liu, H. Liu, S. Zhu, and H. Giessen, Nat. Photonics 3, 157 (2009).

Fig. 1. The BC-SRR orientations and dimensions. The BC-SRR under (a) electrical and (b) magnetic excitation. (c) Vertically and (d) horizontally shifting between two layers. (e) dimensions for a single SRR layer, which forms BC-SRR structure in (f). P=60µm, l=40µm, w=11µm, g=5µm, substrate thickness (t_{sub})=5µm, and superstrate thickness (t_{super})=5µm.
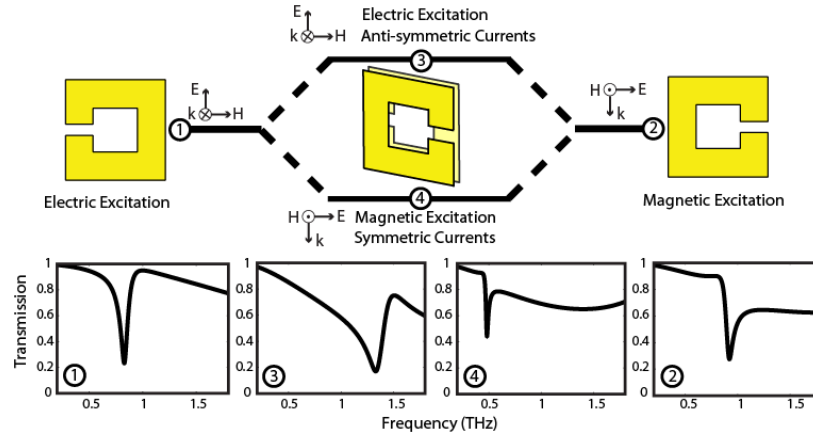
Fig. 2. Hybridization in broadside coupled SRRs. Top panel: For single SRRs within a unit cell, the magnetically and electrically excited modes are degenerate. The broadside configuration leads to hybridization removing the degeneracy leading to an increase (decrease) in the resonance frequency for electric (magnetic) excitation. Lower panel: Full-wave calculations of the transmission for demonstrating splitting of the resonances for BC-SRRs. The dimensions used for the simulation are listed in Fig. 1.
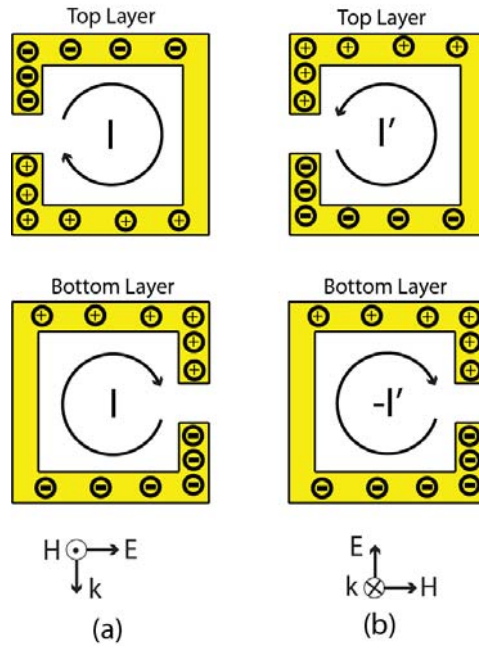
Fig. 3. Schematic views of the surface charge distributions and their corresponding surface current distributions for (a) magnetically and (b) electrically excited BC-SRR structures. The top and bottom layers are shown displaced for clarity.
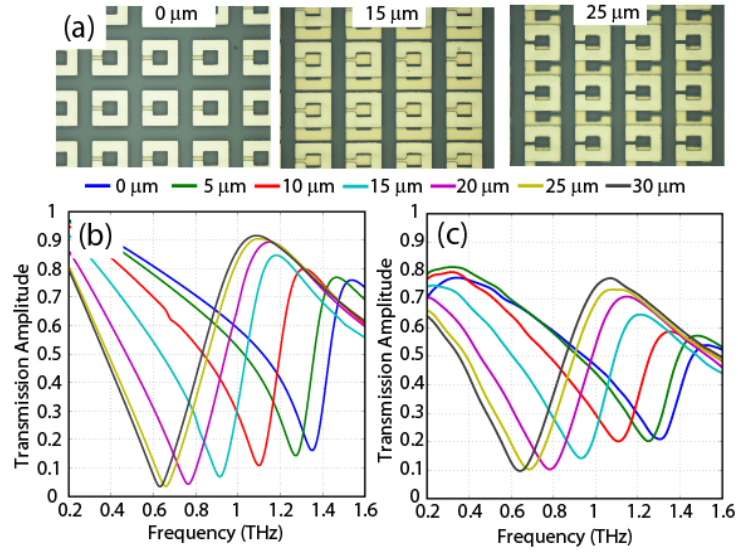
Fig. 4. (a) Optical microscope pictures of BC-SRR structures shifted along vertical direction for 0µm (no-shift), 15µm, and 25µm. (b) Simulation and (c) experimental results for transmission characteristics of BC-SRR structures shifted along vertical direction for 0µm, 5µm, 10µm, 15µm, 20µm, 25µm, and 30µm.
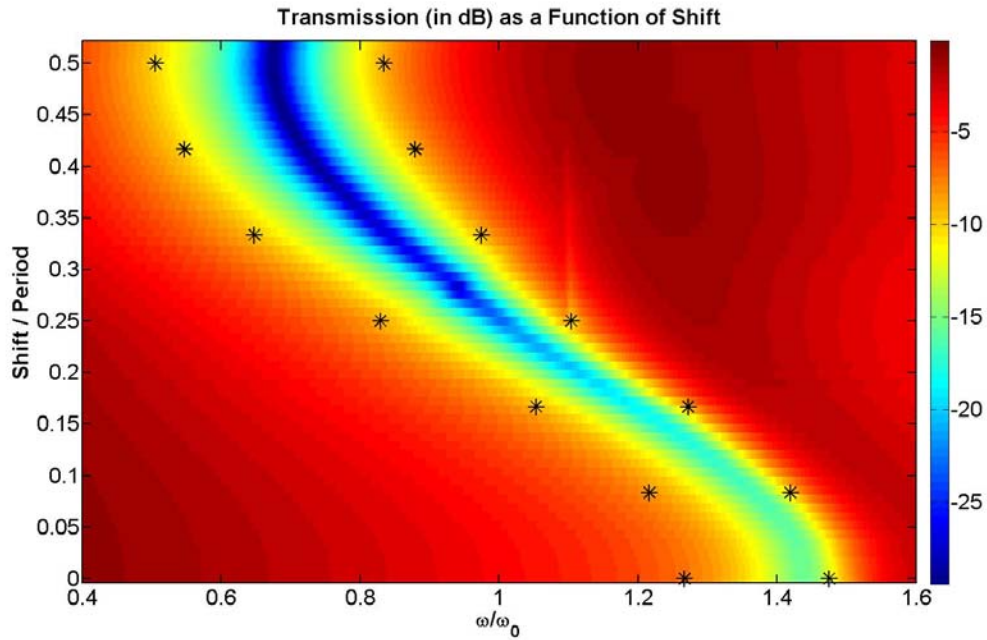
Fig. 5. Broadband transmission of shifted BC-SRR arrays for electrical excitation. The transmission curves were simulations in steps of 0.5μm from 0μm to 30μm. In addition, the overlaid crosses represent the -10dB points from experiment. In contrast to Figure 5 of [24], we excite only a single mode in these arrays. The second mode, if present, would mirror the behavior about the line $\omega/\omega_0 = 1$ [i.e. it would start near ($\omega/\omega_0 = .6$, Shift / Period = 0) and curve up and right towards ($\omega/\omega_0 = 1.3$, Shift / Period = 0.5)]. The figure is plotted in dB for clarity.